Doxorubicin Intracellular Release Via External UV Irradiation of Dextran- g -poly(o -nitrobenzyl acrylate) Photosensitive Nanoparticles

Meriem El Founi, Hamed Laroui, Brandon S.B. Canup, Joseph Ametepe, Régis Vanderesse, Samir Acherar, Jérome Babin, Khalid Ferji, Isabelle Chevalot, Jean-Luc Six

Doxorubicin Intracellular Release *via* External UV Irradiation of dextran-*g*-poly(*o*-nitrobenzyl acrylate) Photosensitive Nanoparticles

Meriem EL FOUNI,[a] Hamed LAROUI[b] Brandon S.B. CANUP,[b] Joseph S. AMETEPE,[b] Régis VANDERESSE,[a] Samir ACHERAR,[a] Jérome BABIN,[a] Khalid FERJI,[a] Isabelle CHEVALOT,[c] Jean-Luc SIX,[a,]*

a) Université de Lorraine, CNRS, LCPM, F-5400 Nancy, France

b) Department of Chemistry/Biology, Georgia State University, Atlanta, GA, United States

c) Université de Lorraine, CNRS, LRGP, F-5400 Nancy, France

Submitted to ACS Applied Bio Materials

ABSTRACT.

In the present study, innovative doxorubicin-loaded NPs made of a photosensitive poly(*o*-nitrobenzyl acrylate) (PNBA) hydrophobic matrix and an hydrophilic dextran (Dex) shell were firstly formulated by emulsion-solvent evaporation process. Doxorubicin (DOX), a very well-known anticancer drug, was herein chosen as model. DOX-loaded NPs were successfully produced by covering the hydrophobic PNBA core with dextran chains either physically adsorbed or covalently linked by changing process parameters as the presence of a catalyst (CuBr or $CuSO_4$/ascorbic acid). It was then proved that the neutralization of DOX optimized the drug loading. DOX drug loading and release were independent of the coverage mechanism if the catalyst used to covalently link the shell to the core was correctly chosen. Secondly, the kinetics of DOX release were investigated by simple diffusion or light-irradiation of the NPs. Experiments showed that less than 20% of DOX were released by simple diffusion after 48 h in PBS or DMEM media when 45% of DOX released after only 30 s of light irradiation of the NPs. Finally, the impact of the photo-triggered DOX release on cells viability was investigated on various cell lines (Caco-2, HepG2, HCT-116, HT-29 cells as well as murine macrophages (RAW 264.7)). Cellular mortality was evaluated to be dependent on the cell lines tested. Our approach provided an improved DOX release towards human liver cancer cell line and a high internalization of the PNBA-based NPs into HepG2 cells was observed using fluorescence microscopy.

KEYWORDS: amphiphilic glycopolymer, drug delivery system, phototherapy, liver cancer, colorectal cancer

I) INTRODUCTION

During many decades, the encapsulation of anticancer drugs into "smart" polymeric nanoparticles (NPs) has grasped great attention in academia. These NPs are prepared from polymers sensitive to endogenous or external stimuli including temperature, pH, and light.[1-6] Within the latter ones, light-irradiation is probably the most attractive external stimulus due to its easy operating conditions, relative low cost, and its spatio/temporally control. This latter characteristic could be very useful as specific light excitation can lead to the swelling/disruption of photosensitive NPs, and consequently to the release of loaded drug at a specific time and place near to a specific organ.[7-12] We reported several promising polymeric NPs, nanocapsules, polymersomes for drug delivery applications.[13-24] Photosensitive NPs based on dextran hydrophilic shell and on poly(*o*-nitrobenzyl acrylate) (PNBA) hydrophobic matrix were recently described and their photosensitive behavior was investigated under UV-irradiation (320nm - 400nm) according the photolysis of PNBA (hydrophobic) to polyacrylic acid (PAA, hydrophilic) (Figure 1).[25] Interestingly, nitrobenzyl esters located into PNBA chains can be photolyzed upon either single-photon UV (*e.g.* 365 nm) or two-photon near-infrared (NIR) (*e.g.* 700 nm).[26-28] The two-photons NIR light allows biomedical treatments of deep tissues when UV irradiation, less "tissue-penetrant", could be directly applied by *in situ* endoscopy.[29] Although micellization of copolymers containing PNBA or poly(*o*-nitrobenzyl methacrylate) (PNBM) block have already been reported,[26, 30-37] only two papers dealt with formulation of NPs based on either PNBA[38] or PNBM[39] core but none reported the potential of such photosensitive NPs for encapsulation of anticancer drugs.

Doxorubicin (DOX, Scheme S1), an anthracycline antibiotic isolated from *Streptomyces strains*, is probably one of the most efficient drugs used to treat various cancers, including

lymphoma, breast, prostate, liver, and colon cancers. Action of DOX follows various mechanisms: i) inhibition of the DNA topoisomerase II and DNA polymerase, ii) intercalation into the DNA helix, and iii) free radical formation, lipid peroxidation, and direct membrane effects.[40] The solubility of this drug is limited to 0.27 g/L in aqueous medium at 6.0 <pH< 7.5, but increases to 0.98 g/L in acidic medium (pH ~ 4).[41] This could be relevant for the cancer treatments *via* chemotherapy as the extracellular pH of tumor reaches 6.8 [40], and internal pH is around 4 in lysosome.[42-43] However, due to the low efficiency of the direct DOX injections, many repetitive injections at regular periods are required which can induce some undesirable effects when long-term is used.[44] Since many decades, encapsulation of DOX into nano-objects has appeared as an efficient pathway to reduce injected doses, to enhance DOX biodistribution, and to improve its pharmacokinetic characteristics.[40, 45] Many commercial suspensions of DOX-loaded nano-objects are currently marketed, *i.e.* DOXIL®, MYOCET®, NUDOXA® or CAELYX®. However, such systems are exclusively based on liposomes which suffer from low mechanical and chemical stabilities and a high membrane permeability due to the dynamic membrane mobility, that can induce a premature drugs leakage.[46-47]

The present study firstly reports a detailed investigation on the encapsulation of DOX into such photosensitive PNBA-based NPs (Figure 1). The influence of various parameters including the chemical form of DOX and catalyst used in the formulation process were evaluated. In this study, two catalysts were compared. The release kinetics of DOX from NPs in PBS and DMEM media were then measured depending on the NPs coverage mechanism, both by simple diffusion through the NPs matrix (without light excitation) and under UV-irradiation according the NPs matrix disruption. The safety of such applied UV-treatment was previously optimized after study on Caco-2 cells (human epithelial colorectal adenocarcinoma) to guarantee 100% of cell

viability.[25] Finally, the *in vitro* ~~drug~~ DOX release was studied towards different model cells including Caco-2, HepG2 (human liver cancer cells), HCT-116 (human colonic carcinoma cells), HT-29 (human colorectal adenocarcinoma cells) and murine macrophages (RAW 264.7). Then, the DOX-loaded PNBA-based NPs uptake was investigated depending on cell lines. To the best of our knowledge, this paper is the first one dealing with the *in vitro* anticancer release from PNBA-based photosensitive NPs as well as with their uptake depending on cell lines.

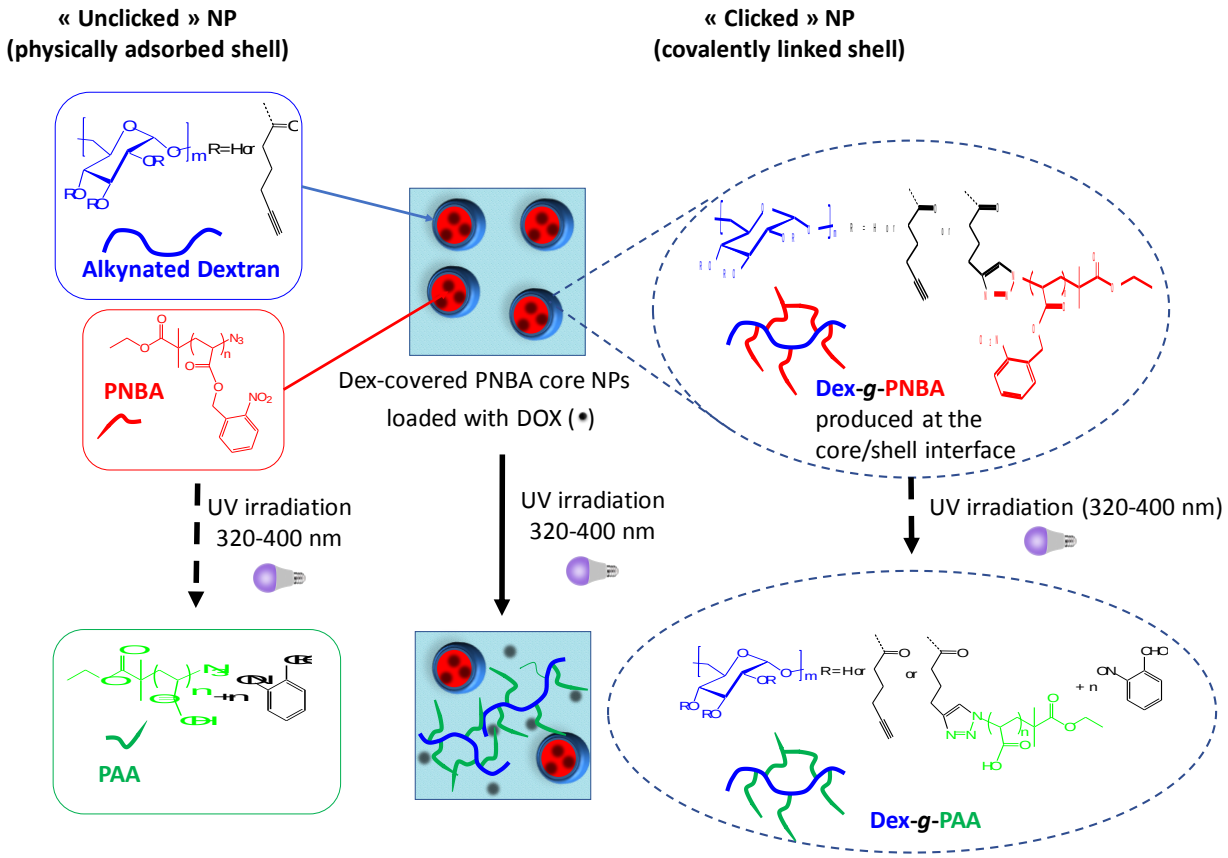

Figure 1. DOX-loaded NPs. UV-irradiation leads to the DOX release due to the progressive NPs core disruption (photolysis of PNBA chains/grafts).

II. EXPERIMENTAL

II.1) Materials

Azido-end functionalized PNBA (called PNBA in the present study, $\overline{M_n}$ = 10 300 g/mol, Đ = 1.24) was obtained by SET-LRP of *o*-nitrobenzyl acrylate as previously reported. [48] Alkynated dextran (15 alkyne groups per 100 glucopyranosic units, $\overline{M_n}$ = 27 500 g/mol, Đ = 1.35) was prepared by modification of Dextran T40 ($\overline{M_n}$ = 26 000 g/mol, Đ = 1.30; purchased from Merck).[49] Doxorubicin hydrochloride (DOX . HCl, > 95 %) was purchased from TCI. Dichloromethane (DCM), triethylamine (NEt_3), copper bromide (CuBr, 99.9%), copper sulphate pentahydrate ($CuSO_4$. $5H_2O$, >98%), *L*-ascorbic acid (AAsc), ethylenediaminetetraacetic acid (EDTA) and terephthalaldehyde were purchased from Merck and used without further purification. Phosphate Buffer Saline (PBS) was prepared as follows: [Na_2HPO_4] = 6.48 mM, [KH_2PO_4] = 1.47 mM, [NaCl] = 138 mM, and [KCl] = 2.68 mM, final pH adjusted to 7.4. Ultrapure deionized water (>18.2 MΩ.cm) was used for the preparation of all solutions. DMEM (Dulbecco modified eagle's medium with high glucose concentration (4.5 g/L), 4 mM *L*-glutamine, supplemented with 10% Fetal Bovine Serum (FBS), and 1% antibiotic antimycotic solution) was purchased from Sigma. Dulbecco's Phosphate Buffered Saline (d-PBS) was purchased from Merck, and Trypsin – EDTA solution was purchased from GIBCO.

II.2) Elaboration of DOX-loaded NPs using an emulsion/solvent evaporation (ESE) process

In a typical experiment, 50 mg of alkynated dextran were dissolved in 10 mL of Milli-Q water (DCM saturated). Meanwhile, the initial organic phase was made by dissolving 25 mg of PNBA and 15 mg of DOX . HCl in 1 mL of DCM. In some specific experiments, 18 µL of NEt_3 (5 eq. per DOX . HCl) were also added to neutralize DOX . HCl according Scheme S1, leading to consider 14.056 mg of DOX as the initial amount of DOX introduced. In case of unloaded NPs,

this initial DCM solution contained only 40 mg of PNBA. The organic phase was finally poured to the aqueous one and the mixture was sonicated during 2 min at 0°C (50% pulsed mode, 46 W) using Vibracell 75 model (Bioblock Scientific). The obtained emulsion was kept under slow stirring during 2.5 h at 37°C to evaporate DCM. Finally, after complete DCM evaporation, "unclicked" NPs were collected by centrifugation (22,000 g, 15 °C, 60 min) and washed twice (resuspended in Milli-Q water then centrifuged again) to remove both the non-adsorbed alkynated dextran and the unloaded DOX.

To formulate "clicked" NPs, 5 eq. of copper catalyst (CuBr or $CuSO_4$/AAsc (1/10)) per PNBA chains were added to the mixture prior the sonication step. After washing steps, EDTA (5 eq. per CuBr or $CuSO_4$) was added to the final washed NPs suspension to remove residual copper and left under slow stirring for 24 h at room temperature. Finally, purified "clicked" NPs were collected as above.

II.3) Determination of the DOX loading and encapsulation efficiency

Drug loading (DL) and encapsulation efficiency (EE) were estimated by ^{1}H NMR spectrum after dissolving known weights of freeze-dried loaded NPs (w_{NPs}) and an internal reference (terephthalaldehyde) in DMSO-d_6, and using Equations 1 and 2, respectively:

$$\mathrm{DL}(\%) = \frac{\text{weight of loaded DOX}}{\text{Total weight of loaded NPs}} \times 100 = \frac{A_d/3}{A_{ref}/2} \times \frac{M_{DOX} \times w_{ref}}{M_{ref} \times w_{NPs}} \times 100 \quad (1)$$

$$\mathrm{EE}(\%) = \frac{\text{weight of loaded DOX}}{\text{weight of DOX feed}} \times 100 = \frac{A_d/3}{A_{ref}/2} \times \frac{M_{DOX} \times w_{ref}}{M_{ref} \times w_{DOX}} \times 100 \quad (2)$$

A_d and A_{ref} are respectively the peak areas of the three methoxy protons of doxorubicin (4.05 ppm) and the two aldehyde protons of terephthalaldehyde (10.15 ppm) (Figure S1). M_{DOX} = 543.48 g/mol and M_{ref} = 134.13 g/mol are respectively the molar masses of neutralized DOX and terephthalaldehyde. w_{ref}, w_{NPs} and w_{DOX} are the weights of terephthalaldehyde, DOX loaded-NPs and DOX used in the initial mix.

II.4) Study of the kinetic of DOX release

The kinetic of DOX release from the NPs were carried out in 96-well microplate either after NPs disruption (upon light irradiation) or by simple diffusion through the matrix (without UV-irradiation). In brief, 20 µL of NPs dispersion (1.25 mg/mL) were introduced per well then 200 µL of PBS or DMEM were added. NPs dispersions were irradiated 30 s, 1 or 3 min (320 nm – 400 nm, irradiance 60 mW/cm^2). Immediately after irradiation, some NPs suspensions were centrifuged (37,000 g, 15°C, 3 min) and the supernatants were analyzed to estimate the released DOX amount using HPLC calibration curves in PBS or DMEM (Figure S2). We spare another batches of NPs suspension from the same synthesis to study the DOX kinetic of release during 48 h.

II.5) Optimization of the DOX solubility

Each medium (PBS and DMEM) was saturated with DOX, left for day in dark under stirring, then the resulted suspension was centrifuged (37,000 g, 15 °C, 45 min). Maximum solubilities of DOX were estimated by UV spectroscopy at 480 nm (Figure S3).

II.6) Cells viability tests to measure cellular biocompatibility of the NPs

Caco-2 cells were kindly provided by the laboratory URAFPA (Nancy, France). These cells were used between passages 30 and 50, and were cultivated in DMEM with high glucose (4.5 g/L) (Sigma, Germany), and supplemented with 10% foetal calf serum (FCS) (EuroBio, France), 2 mM$_L$-glutamine, and 1% nonessential aminoacids (GIBCO, USA). RAW 264.7, HCT-116, HT-29 and HepG2 were cultured in the 1g/L *L*-glutamine DMEM medium with 10% FBS (Denville Scientific), 5% Penicillin and streptomycin (100X Corning) at 37℃. Cells were usually split when reaching 80% confluence (3–4 days), rinsed with d-PBS, then trypsinized with a solution

containing 0.25% trypsin and 1 mM EDTA (GIBCO). Cells were seeded into 96-well microplates adding 200 µL of a suspension of $2x10^4$ cells/well.

After 24 h, cells were incubated with different batches of DOX-loaded NPs dispersion (NPs concentration = 114 µg/mL), then UV-irradiated (up to 30 min). The culture medium was renewed 4 h after the irradiation to remove free DOX, then cells were incubated for another 24 h or 48 h at 37°C under 5% CO_2 as previously described.[25] Cells without UV-irradiation and without addition of NPs were cultivated as controls. After incubation, the released DOX amount was first estimated by HPLC. Then, the culture medium was removed and 200 µL of fresh medium were added. The cell viability was determined by MTT assay, using mitochondrial succinate dehydrogenase activity of viable cells by the reduction of the yellow colored tetrazolium salt, 3-(4,5-dimethylthiazol-2-yl)-2,5-diphenyl tetrazolium bromide, into a blue colored formazan product. More precisely, 50 µL of MTT solution (2 g/L) were added in each well. After incubation for 3 h at 37°C, formazan crystals were observed, dissolved with 150 µL of isopropyl alcohol, then spectrophotometrically quantified at 550 nm using a multi-well plate reader. OD values were used to calculate the percentage of cell viability using Equation (3). All these cytotoxicity experiments were performed in triplicate (n=3). Error bars (see below) represent standard deviation (SD) of the mean value for three independent experiments. One-way ANOVA analysis of variance was performed. Significant differences between means were determined by Duncan's Multiple Range tests. Differences at $p > 0.05$ were considered significant.

$$\text{Percentage of cell viability (\%)} = \frac{OD_{Exp} - OD_{neg\ cont}}{OD_{pos\ cont} - OD_{neg\ cont}} \times 100 \qquad (3)$$

Where OD_{Exp}, $OD_{neg\ cont}$ and $OD_{pos\ cont}$ are the experimental optical density and OD observed for negative (cells without irradiation) and positive (cells with irradiation) controls, respectively.

II. 7) DOX-loaded NPs uptake and *in vitro* DOX release

RAW 264.7, HCT-116, HT-29 and HepG2 were used in the present study. Cells were seeded into chamber slides (Thermo Scientific) and 400 µg/mL of NPs were added into the culture medium. After confluence, cells were incubated with NPs for 4 h, then 30 s UV-irradiation was applied to release the DOX. Cells were washed with d-PBS 3 times to remove free DOX or NPs which were not uptake by cells. Then, cells were fixed by using 4% of paraformaldehyde for 15 min at room temperature. Cells were again washed three times by d-PBS, then Alexa Fluor 568 phalloidin (568 nm, Thermo Scientific) was added to stain the F-actin (Red fluorescence) located into the plasma membrane (red-orange). Cells were also stained with DAPI (350 nm, Thermo Scientific) for 5 min to reveal the cells nuclei (blue-purple).[50] Slides were sealed with prolong gold antifade reagent (Thermo Fisher). Slides were imaged on a fluorescent microscope (Olympus, Shinjuku, Tokyo).

II. 8) Characterizations

^{1}H NMR spectra were recorded on a Bruker Advance 300 spectrometer (300.13 MHz, 298°K) in DMSO-d_6.

Analytic HPLC was performed on a SHIMADZU CTO-20A/Prominence column oven, with LC Solution program Release 1.23 SP1 using a Pursuit C8 column (150 x 4.6, 5 µm) and a linear gradient of water/acetonitrile (v/v) solution (90/10 during 20 min, then 100/0 (v/v) during 10 min) with 1 mL/min flow. The detection was performed at 480 nm using a SHIMADZU SPD20AV/Prominence UV/VIS detector.

Dynamic Light Scattering (DLS) of NPs dispersion at low concentration was evaluated using a Malvern High Performance Particle Sizer (HPPS) instrument. 200 µL of NPs suspension were diluted in 2 mL of NaCl aqueous solution (1 mM). The analysis of the average scattering

intensity fluctuations during the measurement allowed to estimate the NPs size and the polydispersity index (PDI). The average hydrodynamic diameter (Dh) is the so-called Z-average mean diameter (Dz) given from cumulated analysis, *i.e.* an intensity–average diameter, and was measured three times with deviation remaining below 5 nm.

OmniCure® S1000 UV spot cure lamp equipped with a light guide of 8 mm diameter and a 320–400 nm filter was used with an irradiance equal to 60 mW/cm^2.

III. RESULTS AND DISCUSSION

III.1) Doxorubicin encapsulation into photosensitive NPs

The encapsulation of doxorubicin in the PNBA-based NPs was carried out using emulsion/solvent evaporation (ESE) process. Drug loading (DL) and encapsulation efficiency (EE) which are the main parameters to evaluate an encapsulation process, were directly estimated by ^1H NMR spectrum of DOX-loaded NPs (figure S1) using Equations 1 and 2. An important parameter of the ESE process is the total solubilizations of both the drug and the hydrophobic polymer forming the NPs core in a common organic water-immiscible solvent. In the present study, we firstly optimized the encapsulation of doxorubicin in PNBA-based NPs, in its water-soluble salt form (DOX . HCl) and in its hydrophobic form (DOX) after neutralization by NEt_3 (Scheme S1).[51] Table 1 (runs 1-3) shows successful formulation of well-defined NPs (PDI < 0.15), both in the absence and in the presence of doxorubicin. However, an increase of the Z-average diameter was noticed for loaded NPs (159 nm and 275 nm) in comparison with unloaded ones (128 nm) due to the successful encapsulation of doxorubicin. A significant difference of D_Z of NPs was observed depending on the doxorubicin form used. NPs loaded by DOX exhibit higher D_Z (275 nm) compared to NPs loaded by DOX . HCl (159 nm). In addition,

neutralization of DOX . HCl, allowed great improvement of both DL (multiplied by 3) and EE (increased from 18 to 88%). These findings demonstrate that the neutral form of doxorubicin (DOX) is more suitable for an encapsulation within the hydrophobic PNBA core NPs, in agreement with its lower solubility in the aqueous phase and with other results previously reported in the literature.[51]

Table 1. Characterization of the DOX-loaded NPs as a function of the DOX/PNBA weight ratio

Run	$w_{DOX\ .\ HCl}$ / w_{PNBA} (mg/mg) [a]	Doxorubicin form	Z-Average diameter (nm) [b]	PDI [b]	DL (%) [c]	EE (%) [c]
1	0/40	-	128	0.09	-	-
2	15/25	DOX . HCl	159	0.12	10	18
3	15/25	DOX	275 *	0.12 *	33 *	88 *
4	5/35	DOX	177	0.07	9	74
5	10/30	DOX	225	0.09	18	70
6	20/20	DOX	923	0.43	41	74
7 [d]	15/25	DOX	243 *	0.13 *	29 *	73 *
8 [d]	15/25	DOX	149	0.09	11	22

a) DOX . HCl/PNBA weights ratio in the feed

b) Estimated by DLS.

c) DOX loading (DL) and encapsulation efficiency (EE).

d) "Clicked" NPs were formulated using CuBr (run 7) or $CuSO_4$/AAsc catalyst system (run 8).

* from ref [52]

To further complete the DOX loading study, the influence of the quantity of DOX . HCl in the feed on the NPs loading efficiency was secondly investigated. Various weights of DOX . HCl ($w_{DOX,HCl}$) and adequate amount of NEt_3 were introduced in the feed, and the weight of PNBA dissolved in the organic phase was consequently adjusted to keep the same total weight (PNBA + DOX . HCl) of 40 mg in all experiments. Table 1 (runs 3-6) showed an increase of DL from 9 to 41 % with an increasing amount of DOX in the feed. Notably, the EE (88%) was obtained with 15 mg of DOX . HCl in the feed (Table 1, run 3) compared to 74% with 20 mg (Table 1, run 6). It can be assumed that this decrease of EE could be due to the saturation of the PNBA core of NPs that reached the maximum of encapsulation. This statement is consistent with the huge D_Z (923 nm) of particles formulated using 20 mg of DOX . HCl and 20 mg PNBA (Table 1, run 6). Confirming the results, the high PDI measured (0.43) indicates a high formation of aggregates. In contrast, monomodal distributions of NPs were obtained when using lower quantity of doxorubicin (runs 3-5). All our results led us to use the DOX . HCl/PNBA weight ratio of 15/25 for the rest of this study.

Using the above ESE process, NPs were formulated with a physically adsorbed dextran shell onto the core ("unclicked" NPs as drawn in Figure 1). This shell can also be irreversibly anchored on the core by carrying out an *in situ* interfacial click chemistry during this ESE process, leading to "clicked" NPs (Figure 1). This click chemistry leads to produce a covalent linkage between dextran and PNBA parts *via* triazole rings producing Dex-*g*-PNBA copolymers at the interface (Figure 1). Interestingly, while a quantitative surface desorption from the "unclicked" NPs was observed in the presence of a competitive surfactant, the desorption was significantly reduced (around 80% decrease) in case of "clicked" NPs due to this core/shell covalent bonding.[23, 25, 53] Such improved colloidal stability thanks to a covalent bonding is

already reported in many systems, for example for the complexation of polyelectrolytes of opposite charge.[54]

In the present study, "clicked" NPs were then formulated and compared with "unclicked" NPs (Table 1, run 3). Two well-known catalysts (CuBr or $CuSO_4$/AAsc) of the alkyne/azide click chemistry within the ESE process were investigated. As shown in Table 1, monodispersed "clicked" NPs smaller than 250 nm (PDI < 0.15) were formulated. CuBr (Table 1, run 7) led to similar DL and EE values than the ones of "unclicked" NPs (Table 1, run 3). Notably, $CuSO_4$/AAsc catalyst system strongly decreased the DOX encapsulation (decrease of 2/3 in DL) (Table 1, run 8). For the first time, these results suggest that CuBr as catalyst does not influence the DOX loading in PNBA core. In contrast, the presence of AAsc decreases the pH of the aqueous phase to 3.5, which leads to the DOX protonation. As mentioned before, the protonated DOX has a lower loading efficiency in the formulation method.

III.2) Quantification of DOX released by diffusion

Before investigating the influence of the medium (PBS or DMEM) on the DOX release, the maximum DOX solubility in each medium were determined. Our experiments show that DOX is less soluble in DMEM (186 μM, 0.101 mg/mL) compared to PBS (1066 μM, 0.579 mg/mL). This can probably be explained by the complex composition of foetal bovine serum used to supplement DMEM medium (notably the presence of bovine serum albumin). Thus, experimental conditions of release were chosen regarding theses difference of solubility, in order to fix the DOX concentration below saturation of the medium (typically 10% of the maximum concentration).

DOX release was firstly investigated by simple diffusion from the NPs at 37°C during 2 days (Figure 2A). On the one hand, it was noticed that the "clicked" and "unclicked" NPs batches

(Table 1, runs 3, 7 and 8) exhibited similar kinetics profile of release. On the other hand, a very slow release was observed (20% after 48 hours). More importantly, for all conditions, DOX release was performed without burst effect, demonstrating that DOX was uniformly encapsulated in the PNBA core of NPs and the absence of a significant DOX adsorption at the NPs surface.

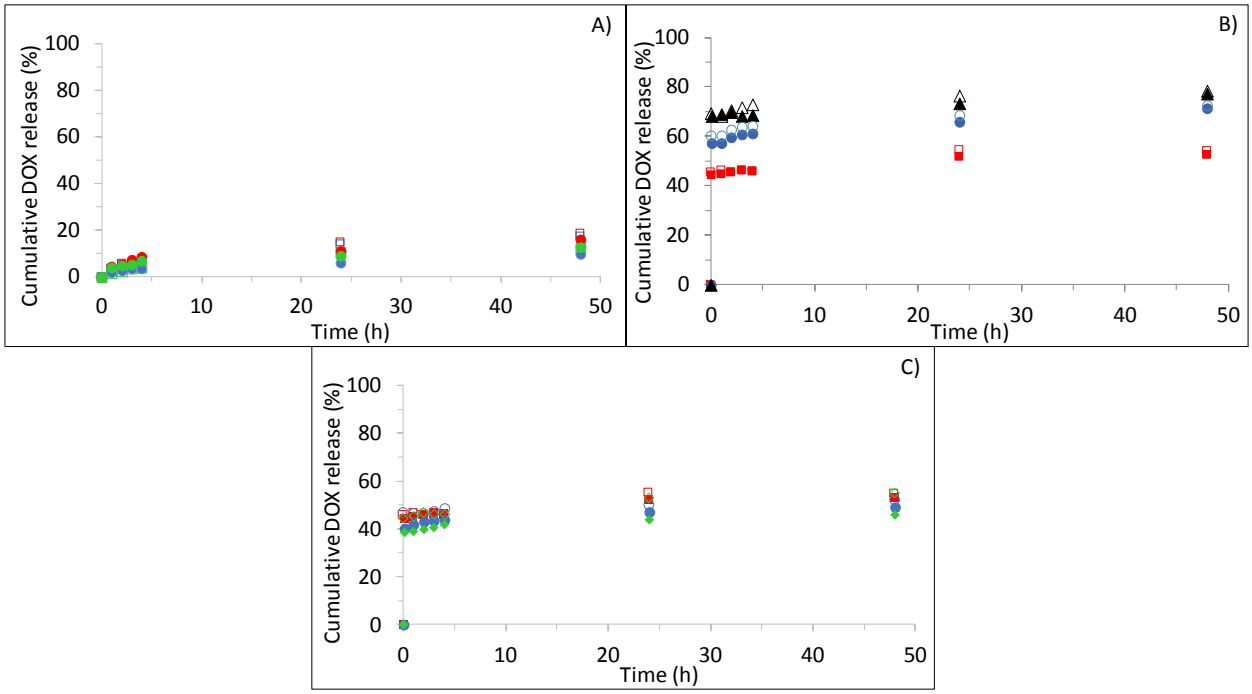

Figure 2. Cumulative DOX release from PNBA-based NPs in DMEM (solid symbols) or PBS (open symbols). A) By diffusion from "clicked" or "unclicked" NPs (red symbols = run 3, blue symbols = run 7, green symbols = run 8, Table 1). B) With "unclicked" NPs (Table 1, run 3), under UV-irradiation during 30 s (red symbols), 1 min (blue symbols) or 3 min (black symbols). C) Under UV-irradiation during 30 s (red symbols = run 3, blue symbols = run 7, green symbols = run 8, Table 1).

III.3) Light-triggered release of the DOX

According to our previous results on the loading/release of Nile Red (hydrophobic fluorescent probe) from PNBA-based NPs[52], DOX release could be light-triggered using the photo-

sensitivity of the PNBA core of the NPs [25] as described in Figure 1. "Unclicked" NPs dispersion was firstly irradiated for several irradiation times (Table 1, run 3). The released DOX amount was quantified by HPLC directly after the irradiation, then followed at several time during 48 h. As shown in Figure 2B, the kinetic of release depends on the irradiation time (30 s, 1 or 3 min of irradiation) and similar profiles were obtained in PBS and DMEM while the DOX solubility in DMEM is nearly six times lower as above written. 18% of the loaded DOX were released by diffusion (without irradiation) after 48 h, whereas 45 % of release was observed immediately after 30 s irradiation. In this latter condition, the post-irradiation release of DOX reached almost 54 % after 48 h diffusion (33 µM of DOX, which is the DOX IC_{50} towards Caco-2 cells as reported in Figure S4). 78% of DOX release was reached using 3 min irradiation then 48 h diffusion. The longer the irradiation time, the greater the amount of DOX released, in accordance with the progressive photolysis/disruption of the PNBA NPs matrix. In order to study the impact of the coverage of the NPs ("unclicked" and "clicked"), DOX-loaded NPs were irradiated during 30 s (Table 1, runs 3, 7-8) then the DOX release was followed during 48 h. As shown in Figure 2C, similar release profiles were observed in PBS and DMEM, for both types of NPs ("unclicked" and "clicked"). These results demonstrate for the first time that the covalent linkage of dextran to the PNBA core does not impact the efficiency of anticancer release from these photosensitive NPs.

III.4) DOX release effect on cells viability

Previously, we have shown that 100% of Caco-2 cells viability was maintained after 48 h incubation with empty PNBA-based NPs and 30 s irradiation with an irradiance of 60 mW/cm^2.[25] Similar results were herein confirmed towards RAW 264.7, HCT-116, HT-29, and HepG2 cell

lines (data used as negative control). All these assays ensure the absence of cytotoxicity of the applied treatment using photosensitive PNBA-based NPs.

Contrary to our previous work, the DOX release effect on the Caco-2 cells viability was herein firstly studied. After UV-irradiation (up to 3 min), cells were left for 4 h incubation before refreshing the medium, then cells were again incubated for another 24 h or 48 h at 37°C. Several DOX-loaded PNBA-based NPs batches (Table 1, runs 3, 7 – 8) were selected to carry out these assays, and results are shown in Figure 3 (0 s of irradiation means DOX release by simple diffusion). Caco-2 cells supplemented with NPs and without irradiation treatment were considered as negative controls.

In agreement with the low DOX diffusion through the NPs without irradiation (DOX concentration estimated at 7 µM by HPLC, Figure 2A), only 20% of Caco-2 cells death was observed after 24 h incubation (meaning 4 h incubation + DMEM refreshing + 24 h incubation), whatever the NPs batch. Comparably, the cells death increased to about 25% after 48 h incubation (Figure S5).

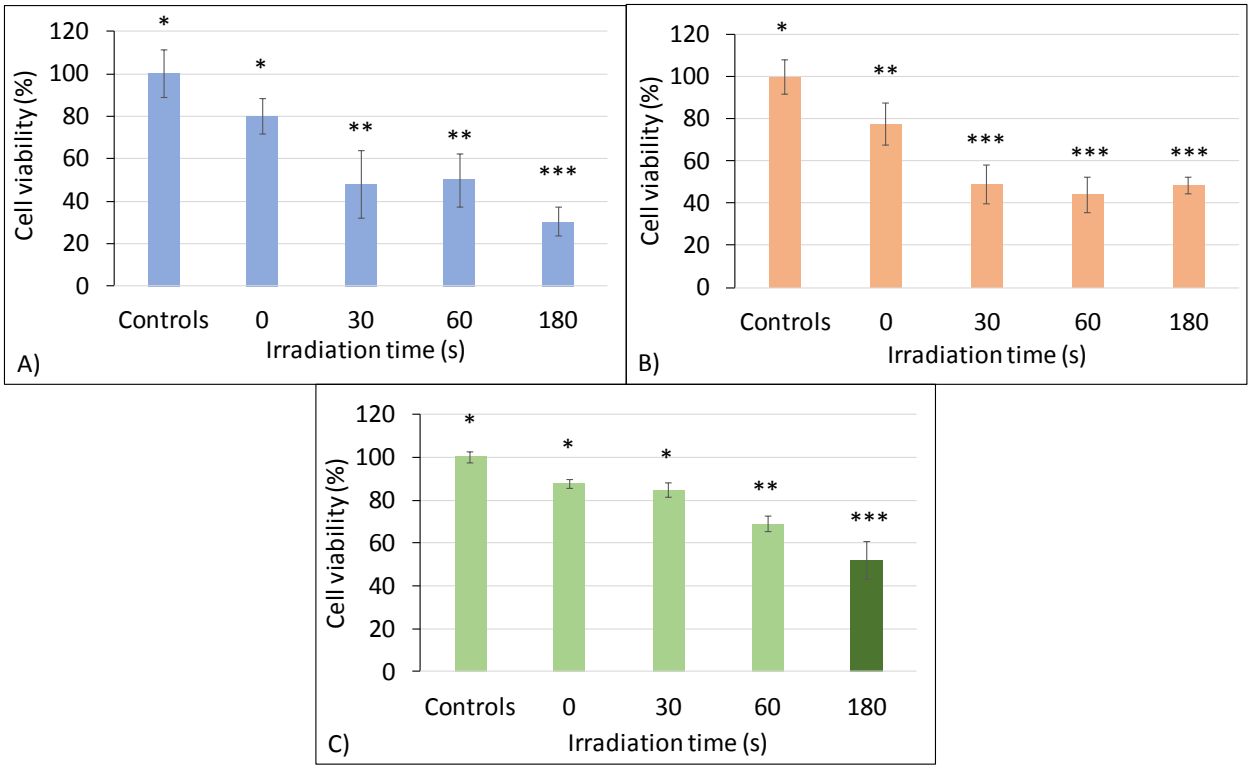

Figure 3. Effect of the photo-triggered DOX release from NPs on the viability of Caco-2 cells after 24 h incubation. Cases of runs 3 (A), run 7 (B) and run 8 (C) (Table 1). Different values are significantly different at the 0.05% level (Duncan's test).

As expected, irradiation of "unclicked" and "clicked" NPs (Table 1, runs 3 and 7) dramatically increased the cells death due to the DOX release from the NPs. Applying 30 s or 1 min of irradiation, cells viability felt out to around 50% after 24 h incubation, in agreement with the photo-triggered release of the DOX (32.5 µM after 30 s; 41.6 µM after 1 min, as estimated by HPLC). These results were consistent with the DOX IC_{50} towards Caco-2 cells estimated around 33 µM (Figure S4). Applying 3 min of irradiation, the cells viability did not exceed 30% in case of "unclicked" NPs (Table 1, run 3), that we can relate to the 46.3 µM of DOX released measured by HPLC after such irradiation time. Nevertheless, the effect of the light-triggered

DOX release from "clicked" NPs formulated using $CuSO_4$/AAsc as catalyst system (Table 1, run 8) was delayed due to the lower DL value of this NPs batch.

From these experiments, we observed for the first time that PNBA-core NPs can significantly improve the “remote” control of the DOX release. This release is indeed not influenced by the method used to fix the shell onto the NPs core (physically adsorbed or covalently linked shell) but depends on the irradiation time. Thus, for NPs with DL around 30%, 30 s irradiation were enough to release 31 µM of DOX, close to the IC_{50} value, reaching 50% of Caco-2 cells death after 24 h incubation. As shown in Figure S5, the simple DOX diffusion from NPs (without irradiation) does not reach such value even after 48 h incubation (10 µM of released DOX in case of "unclicked" NPs was measured) leading to a cell viability around 30%.

These selected NPs (Table 1, runs 3, 7 and 8) were finally also tested by several mammalian cells of interest for potential applications. RAW 264.7, HepG2, HT-29, HCT-116 cells were incubated with 400 µg/mL of NPs for 4 h, then irradiated during 30 s (Figure 4). In this context, we saw that

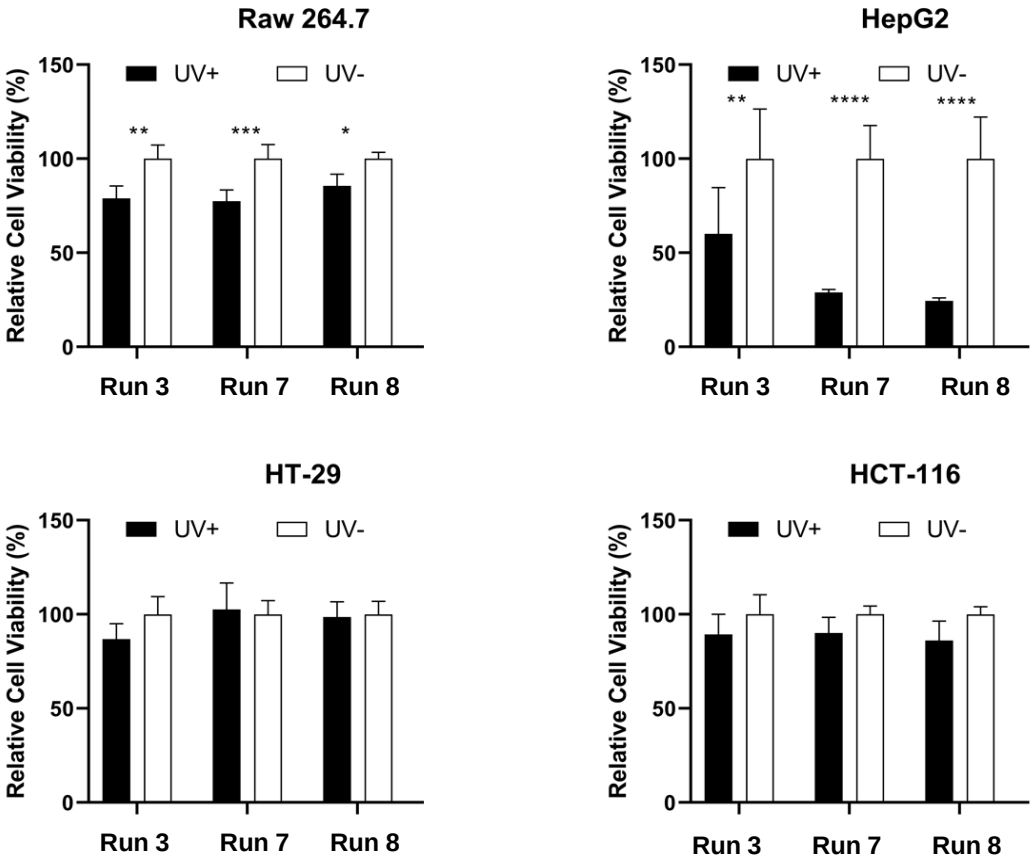

Figure 4. Effect of the photo-triggered DOX release from PNBA-based NPs (Table 1, runs 3, 7 and 8) on the viability on RAW 264.7, HepG2, HT-29, and HCT-116 cells after 4h incubation. Data presented as 30 s UV exposed (UV+) and UV unexposed (UV-). Values represent means ± SE. Data are representative of n=5 wells per group. ***p< 0.001, ** p < 0.01, and * p < 0.05.

the dose of DOX photo-released inside the cells was not high enough to guarantee significant HT-29 and HCT-116 cell death (Figure 4). Treatments with such photosensitive PNBA-based NPs exhibited a moderate degree of cell death on RAW 264.7 cells. Interestingly, among all the cells tested, we observed that HepG2 cells were the most sensitive to DOX photo-triggered release. The HepG2 cells viability was reduced by 50% in case of "unclicked" NPs. On the other

hand, both "clicked" NPs batches led to 75% HepG2 cells death, which confirm for the first time the great potentiality of therapeutic uses of these dextran-covered PNBA-based photosensitive NPs for the liver. We also shown for the first time the influence of the coverage type on the intracellular domain release.

III.5) NPs uptake and intracellular delivery of DOX

To end the present study, "unclicked" and "clicked" DOX-loaded NPs (Table 1, runs 3, 7 and 8) were herein selected to carry out uptake assays. HepG2, HT-29, HCT-116 cancer cells, as well as murine macrophages (RAW 264.7) were incubated with 400 µg/mL of NPs for 4 h, then irradiated during 30 s. The goal of this experiment was to explore a relative short cells exposure to NPs (4 h) to highlight for the first time the efficiency of such potential treatment using photo-triggered DOX released *via* PNBA-based NPs. The short time sets a limiting condition as the cells have a relative short time of endocytosis.

To confirm the DOX was successfully delivered to the recipient RAW 264.7, HepG2, HT-29, and HCT-119 cells, fluorescent microscopy was performed (Figure 5) thanks to DOX fluorescence signal (λ_{em} = 595 nm; λ_{exc} = 470 nm). F-actin located into the plasma membrane was stained with Alexa Fluor 568 phalloidin (red-orange signal) and cells nuclei with DAPI (blue signal). As seen in Figure 5, applying 30 s irradiation treatment, DOX signal was found in all cells UV-treated indicating that DOX was successfully delivered to the cells. HT-29 and HCT-116 present a moderate degree of DOX signal for such treatments. The highest degree of uptake can be seen for the HepG2 cells which may account for the cytotoxicity study in Figure 4.

Interestingly, in case of RAW 264.7 macrophages, the DOX green signal was lower according a few NPs uptake. This significant result represents a huge advantage as avoiding the NPs clearance by macrophages after intravenously administration is one of the key parameters for

reaching efficient cancer treatment. Nevertheless, these results being observed on RAW 264.7 cells, it will need to be confirmed *in vivo* with circulating macrophages from the blood.

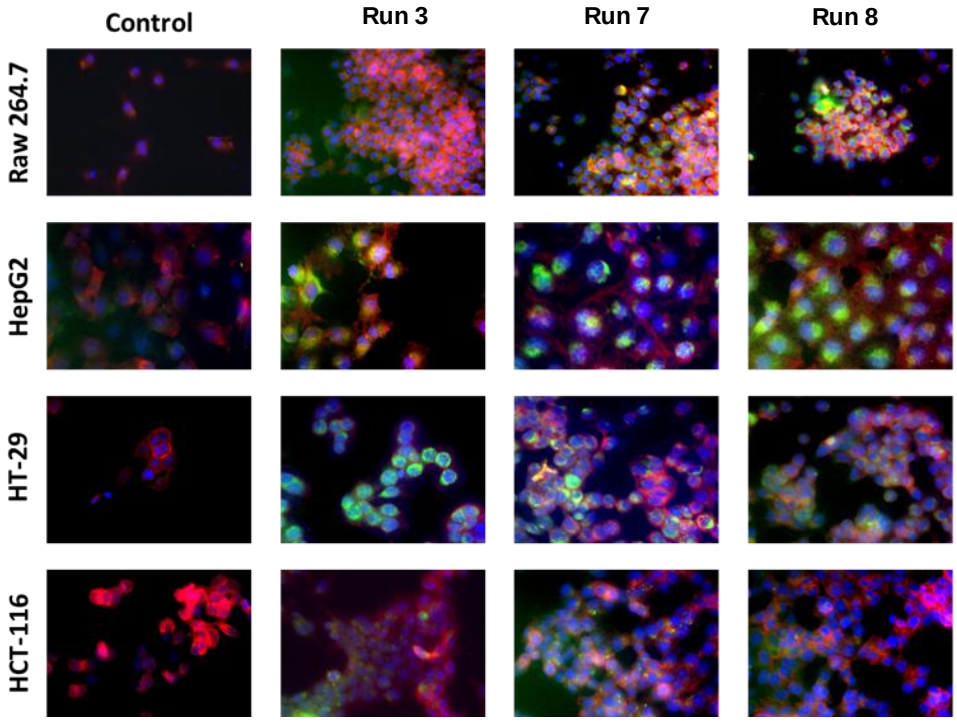

Figure 5. DOX-loaded PNBA-based NPs uptake and intracellular DOX release after 30 s of UV exposure on RAW 264.7, HepG2, HT-29, and HCT-116 cells after 4h incubation (Table 1, runs 3, 7 and 8). Red: Actin stain, Blue: DAPI, and Green: DOX.

IV. CONCLUSION

DOX-loaded dextran-covered PNBA-based NPs were successfully formulated with an emulsion/organic evaporation process. The neutralization of DOX . HCl before encapsulation led to triple the DL (30%) and to load more than 75% of the doxorubicin introduced in the feed (EE).

It was observed that doxorubicin diffused out slowly from these photosensitive NPs in PBS or DMEM medium, without significant influence of the medium. Interestingly, the release can be controlled and accelerated upon UV-irradiation due to the light-triggered disruption of these NPs matrix. Using this strategy, 45% of DOX was released after 30 s UV-irradiation, reaching even 54% if followed by 48 h diffusion, whatever the coverage of the NPs (physically adsorbed or covalently linked shell). As comparison, only 18% of DOX were released after 48 h, without UV-irradiation of NPs, by simple diffusion.

DOX-loaded NPs were then incubated with Caco-2 cells, then irradiated for different times. It was measured that 30 s irradiation were enough to release 31 μM of DOX, which is close to the DOX IC_{50} value towards Caco-2 cells. As comparison, the simple DOX diffusion out of these NPs (without irradiation) does not reach such a result even after 48 h incubation. Cell viability assays were also done on several cancer cells (HepG2, HT-29, and HCT-116) as well as murine macrophages. The photo-released DOX amount was not enough to guarantee significant HT-29 and HCT-116 cells death, when a moderate degree of death was observed with RAW 264.7 cells and up to 75% death with HepG2 cells. A final experiment aimed to measure the efficiency of the NPs uptake by HepG2, HT-29, and HCT-116 and RAW 264.7. As never reported before, it showed that these NPs were particularly highly uptake by HepG2 in comparison with other cells and particularly RAW 264.7. These important results set our engineered DOX-loaded photosensitive Dex/PNBA NPs a potential efficient treatment for liver cancer as avoiding the NPs clearance by macrophages is one of the key parameters for reaching efficient cancer treatment. Nevertheless, more studies have to been done to understand the mechanism of the PNBA-based photosensitive NPs uptake by such HepG2 cells.

V. SUPPLEMENTARY MATERIAL

Supplementary material related to this article can be found in the online version. Neutralization of doxorubicin hydrochloride. ^{1}H NMR spectra of doxorubicin, empty or DOX-loaded PNBA-based NPs. Calibration curves. Determination of DOX IC_{50} towards Caco-2 cells. Effect of the photo-triggered DOX release out of NPs on the Caco-2 cells cytotoxicity after 48 h incubation.

VI. ACKNOWLEDGMENT

M. El Founi was supported by a grant of the French Ministry in charge of Research. The authors express their highest gratitude to Olivier Fabre (LCPM) for NMR measurements, to Jean-Claude Sivault (LCPM) for UV-irradiation apparatus and to Bruno Ebel (LRGP) for statistical analyses.

Corresponding Author

* Corresponding author. E-mail address: jean-luc.six@univ-lorraine.fr

Author Contributions

The manuscript was written through contributions of all authors. All authors have given approval to the final version of the manuscript.

REFERENCES

1. Dai, S.; Ravi, P.; Tam, K. C., Thermo- and photo-responsive polymeric systems. *Soft Matter* **2009,** *5* (13), 2513-2533.
2. Jochum, F. D.; Theato, P., Temperature- and light-responsive smart polymer materials. *Chemical Society Reviews* **2013,** *42* (17), 7468-7483.
3. Karimi, M.; Ghasemi, A.; Sahandi Zangabad, P.; Rahighi, R.; Moosavi Basri, S. M.; Mirshekari, H.; Amiri, M.; Shafaei Pishabad, Z.; Aslani, A.; Bozorgomid, M.; Ghosh, D.; Beyzavi, A.; Vaseghi, A.; Aref, A. R.; Haghani, L.; Bahrami, S.; Hamblin, M. R., Smart micro/nanoparticles in stimulus-responsive drug/gene delivery systems. *Chemical Society Reviews* **2016,** *45* (5), 1457-1501.
4. Liu, D.; Yang, F.; Xiong, F.; Gu, N., The Smart Drug Delivery System and Its Clinical Potential. *Theranostics* **2016,** *6* (9), 1306-1323.
5. Rapoport, N., Physical stimuli-responsive polymeric micelles for anti-cancer drug delivery. *Progress in Polymer Science* **2007,** *32* (8), 962-990.
6. Kost, J.; Langer, R., RESPONSIVE POLYMERIC DELIVERY SYSTEMS. *Adv. Drug Deliv. Rev.* **1991,** *6* (1), 19-50.
7. Bertrand, O.; Gohy, J. F., Photo-responsive polymers: synthesis and applications. *Polymer Chemistry* **2016,** *8* (1), 52-73.
8. Huang, Y.; Dong, R.; Zhu, X.; Yan, D., Photo-responsive polymeric micelles. *Soft Matter* **2014,** *10* (33), 6121-6138.
9. Liu, G.; Liu, W.; Dong, C.-M., UV- and NIR-responsive polymeric nanomedicines for on-demand drug delivery. *Polymer Chemistry* **2013,** *4* (12), 3431-3443.
10. Xiao, P.; Zhang, J.; Zhao, J.; Stenzel, M. H., Light-induced release of molecules from polymers. *Progress in Polymer Science* **2017,** *74*, 1-33.
11. Yan, Q.; Han, D.; Zhao, Y., Main-chain photoresponsive polymers with controlled location of light-cleavable units: from synthetic strategies to structural engineering. *Polymer Chemistry* **2013,** *4* (19), 5026-5037.
12. Zhou, Y.; Ye, H.; Chen, Y.; Zhu, R.; Yin, L., Photoresponsive Drug/Gene Delivery Systems. *Biomacromolecules* **2018,** *19* (6), 1840-1857.
13. Canup, B. S. B.; Song, H.; Le Ngo, V.; Meng, X.; Denning, T. L.; Garg, P.; Laroui, H., CD98 siRNA-loaded nanoparticles decrease hepatic steatosis in mice. *Digestive and liver disease : official journal of the Italian Society of Gastroenterology and the Italian Association for the Study of the Liver* **2012,** *49* (2), 188-196.
14. Ferji, K.; Nouvel, C.; Babin, J.; Li, M.-H.; Gaillard, C.; Nicol, E.; Chassenieux, C.; Six, J.-L., Polymersomes from Amphiphilic Glycopolymers Containing Polymeric Liquid Crystal Grafts. *ACS Macro Letters* **2015,** *4* (10), 1119-1122.
15. Ferji, K.; Venturini, P.; Cleymand, F.; Chassenieux, C.; Six, J.-L., In situ glyco-nanostructure formulation via photo-polymerization induced self-assembly. *Polymer Chemistry* **2018,** *9* (21), 2868-2872.
16. Forero Ramirez, L. M.; Babin, J.; Boudier, A.; Gaucher, C.; Schmutz, M.; Er-Rafik, M.; Durand, A.; Six, J.-L.; Nouvel, C., First multi-reactive polysaccharide-based transurf to produce potentially biocompatible dextran-covered nanocapsules. *Carbohydrate Polymers* **2019,** *224*, 115153.
17. Forero Ramirez, L. M.; Babin, J.; Schmutz, M.; Durand, A.; Six, J.-L.; Nouvel, C., Multi-reactive surfactant and miniemulsion Atom Transfer Radical Polymerization: An elegant controlled one-step way to obtain dextran-covered nanocapsules. *European Polymer Journal* **2018,** *109*, 317-325.

18. Forero Ramirez, L. M.; Boudier, A.; Gaucher, C.; Babin, J.; Durand, A.; Six, J.-L.; Nouvel, C., Dextran-covered pH-sensitive oily core nanocapsules produced by interfacial Reversible Addition-Fragmentation chain transfer miniemulsion polymerization. *Journal of Colloid and Interface Science* **2020,** *569*, 57-67.
19. Ikkene, D.; Arteni, A. A.; Song, H.; Laroui, H.; Six, J. L.; Ferji, K., Synthesis of dextran-based chain transfer agent for RAFT-mediated polymerization and glyco-nanoobjects formulation. *Carbohydrate Polymers* **2020,** *234*, 115943.
20. Laroui, H.; Grossin, L.; Léonard, M.; Stoltz, J.-F.; Gillet, P.; Netter, P.; Dellacherie, E., Hyaluronate-Covered Nanoparticles for the Therapeutic Targeting of Cartilage. *Biomacromolecules* **2007,** *8* (12), 3879-3885.
21. Laroui, H.; Viennois, E.; Xiao, B.; Canup, B. S. B.; Geem, D.; Denning, T. L.; Merlin, D., Fab'-bearing siRNA TNFÎ±-loaded nanoparticles targeted to colonic macrophages offer an effective therapy for experimental colitis. *Journal of Controlled Release* **2014,** *186*, 41-53.
22. Laville, M.; Babin, J. r. m.; Londono, I.; Legros, M. l.; Nouvel, C. c.; Durand, A.; Vanderesse, R. g.; Leonard, M. l.; Six, J.-L., Polysaccharide-covered nanoparticles with improved shell stability using click-chemistry strategies. *Carbohydrate Polymers* **2013,** *93* (2), 537-546.
23. Poltorak, K.; Durand, A.; Léonard, M.; Six, J.-L.; Nouvel, C., Interfacial click chemistry for improving both dextran shell density and stability of biocompatible nanocapsules. *Colloids and Surfaces A: Physicochemical and Engineering Aspects* **2015,** *483*, 8-17.
24. Six, J.-L.; Ferji, K., Polymerization induced self-assembly: an opportunity toward the self-assembly of polysaccharide-containing copolymers into high-order morphologies. *Polymer Chemistry* **2019,** *10* (1), 45-53.
25. El Founi, M.; Soliman, S. M. A.; Vanderesse, R.; Acherar, S.; Guedon, E.; Chevalot, I.; Babin, J.; Six, J.-L., Light-sensitive dextran-covered PNBA nanoparticles as triggered drug delivery systems: Formulation, characteristics and cytotoxicity. *Journal of Colloid and Interface Science* **2018,** *514*, 289-298.
26. Jiang, J.; Tong, X.; Morris, D.; Zhao, Y., Toward Photocontrolled Release Using Light-Dissociable Block Copolymer Micelles. *Macromolecules* **2006,** *39* (13), 4633-4640.
27. Shigenaga, A.; Yamamoto, J.; Sumikawa, Y.; Furuta, T.; Otaka, A., Development and photo-responsive peptide bond cleavage reaction of two-photon near-infrared excitation-responsive peptide. *Tetrahedron Letters* **2010,** *51* (21), 2868-2871.
28. Zhao, H.; Sterner, E. S.; Coughlin, E. B.; Theato, P., o-Nitrobenzyl Alcohol Derivatives: Opportunities in Polymer and Materials Science. *Macromolecules* **2012,** *45* (4), 1723-1736.
29. Suo, Y.; Wu, F.; Xu, P.; Shi, H.; Wang, T.; Liu, H.; Cheng, Z., NIR-II Fluorescence Endoscopy for Targeted Imaging of Colorectal Cancer. *Advanced Healthcare Materials* **2019,** *8* (23), 1900974.
30. Huo, H.; Ma, X.; Dong, Y.; Qu, F., Light/temperature dual-responsive ABC miktoarm star terpolymer micelles for controlled release. *European Polymer Journal* **2017,** *87*, 331-343.
31. Xie, M.; Yu, L.; Li, Z.; Zheng, Z.; Wang, X., Synthesis and character of novel polycarbonate for constructing biodegradable multi-stimuli responsive delivery system. *Journal of Polymer Science Part A: Polymer Chemistry* **2016,** *54* (22), 3583-3592.
32. Shrivastava, S.; Matsuoka, H., Photocleavable amphiphilic diblock copolymer micelles bearing a nitrobenzene block. *Colloid and Polymer Science* **2016,** *294* (5), 879-887.
33. Jana, S.; Saha, A.; Paira, T. K.; Mandal, T. K., Synthesis and Self-Aggregation of Poly(2-ethyl-2-oxazoline)-Based Photocleavable Block Copolymer: Micelle, Compound Micelle,

Reverse Micelle, and Dye Encapsulation/Release. *The Journal of Physical Chemistry B* **2016,** *120* (4), 813-824.
34. Wu, W.-C.; Kuo, Y.-S.; Cheng, C.-H., Dual-stimuli responsive polymeric micelles: preparation, characterization, and controlled drug release. *Journal of Polymer Research* **2015,** *22* (5), 80.
35. Yang, F.; Cao, Z.; Wang, G., Micellar assembly of a photo- and temperature-responsive amphiphilic block copolymer for controlled release. *Polymer Chemistry* **2015,** *6* (46), 7995-8002.
36. Sedlacek, O.; Filippov, S. K.; Svec, P.; Hruby, M., SET-LRP Synthesis of Well-Defined Light-Responsible Block Copolymer Micelles. *Macromolecular Chemistry and Physics* **2019,** *220* (19), 1900238.
37. Hou, W.; Liu, R.; Bi, S.; He, Q.; Wang, H.; Gu, J., Photo-Responsive Polymersomes as Drug Delivery System for Potential Medical Applications. *Molecules* **2020,** *25* (21).
38. Xu, Z.; Yan, B.; Riordon, J.; Zhao, Y.; Sinton, D.; Moffitt, M. G., Microfluidic Synthesis of Photoresponsive Spool-Like Block Copolymer Nanoparticles: Flow-Directed Formation and Light-Triggered Dissociation. *Chemistry of Materials* **2015,** *27* (23), 8094-8104.
39. Cao, Z.; Wu, H.; Dong, J.; Wang, G., Quadruple-Stimuli-Sensitive Polymeric Nanocarriers for Controlled Release under Combined Stimulation. *Macromolecules* **2014,** *47* (24), 8777-8783.
40. Li, J.; Zhang, B.; Yue, C. W.; Wu, J.; Zhao, L. X.; Sun, D. Q.; Wang, R. M., Strategies to release doxorubicin from doxorubicin delivery vehicles. *J. Drug Target.* **2018,** *26* (1), 9-26.
41. Mayer, L. D.; Tai, L. C. L.; Bally, M. B.; Mitilenes, G. N.; Ginsberg, R. S.; Cullis, P. R., Characterization of liposomal systems containing doxorubicin entrapped in response to pH gradients. *Biochimica et Biophysica Acta (BBA) - Biomembranes* **1990,** *1025* (2), 143-151.
42. Liu, J.; Huang, Y.; Kumar, A.; Tan, A.; Jin, S.; Mozhi, A.; Liang, X.-J., pH-Sensitive nano-systems for drug delivery in cancer therapy. *Biotechnology Advances* **2014,** *32* (4), 693-710.
43. Mahoney, B. P.; Raghunand, N.; Baggett, B.; Gillies, R. J., Tumor acidity, ion trapping and chemotherapeutics: I. Acid pH affects the distribution of chemotherapeutic agents in vitro. *Biochemical Pharmacology* **2003,** *66* (7), 1207-1218.
44. Tacar, O.; Sriamornsak, P.; Dass, C. R., Doxorubicin: an update on anticancer molecular action, toxicity and novel drug delivery systems. *Journal of Pharmacy and Pharmacology* **2013,** *65* (2), 157-170.
45. Tardi, P.; Boman, N.; Cullis, P., Liposomal Doxorubicin. *J. Drug Target.* **1996,** *4* (3), 129-140.
46. Chandrawati, R.; Caruso, F., Biomimetic Liposome- and Polymersome-Based Multicompartmentalized Assemblies. *Langmuir* **2012,** *28* (39), 13798-13807.
47. Rideau, E.; Dimova, R.; Schwille, P.; Wurm, F. R.; Landfester, K., Liposomes and polymersomes: a comparative review towards cell mimicking. *Chemical Society Reviews* **2018,** *47* (23), 8572-8610.
48. Soliman, S. M. A.; Nouvel, C.; Babin, J.; Six, J.-L., o-nitrobenzyl acrylate is polymerizable by single electron transfer-living radical polymerization. *Journal of Polymer Science Part A: Polymer Chemistry* **2014,** *52* (15), 2192-2201.
49. Soliman, S. M. A.; Colombeau, L.; Nouvel, C.; Babin, J.; Six, J.-L., Amphiphilic photosensitive dextran-g-poly(o-nitrobenzyl acrylate) glycopolymers. *Carbohydrate Polymers* **2016,** *136*, 598-608.

50. Laroui, H.; Theiss, A. L.; Yan, Y.; Dalmasso, G.; Nguyen, H. T. T.; Sitaraman, S. V.; Merlin, D., Functional TNFÎ± gene silencing mediated by polyethyleneimine/TNFÎ± siRNA nanocomplexes in inflamed colon. *Biomaterials* **2011,** *32* (4), 1218-1228.
51. Sanson, C.; Schatz, C.; Le Meins, J.-F.; Soum, A.; Thévenot, J.; Garanger, E.; Lecommandoux, S., A simple method to achieve high doxorubicin loading in biodegradable polymersomes. *Journal of Controlled Release* **2010,** *147* (3), 428-435.
52. Soliman, S. M. A.; El Founi, M.; Vanderesse, R.; Acherar, S.; Ferji, K.; Babin, J.; Six, J.-L., Light-sensitive dextran-covered PNBA nanoparticles to continuously or discontinuously improve the drug release. *Colloids and Surfaces B: Biointerfaces* **2019,** *182*, 110393.
53. Roy, A.; Murcia Valderrama, M. A.; Daujat, V.; Ferji, K.; Léonard, M.; Durand, A.; Babin, J.; Six, J.-L., Stability of a biodegradable microcarrier surface: physically adsorbed versus chemically linked shells. *Journal of Materials Chemistry B* **2018,** *6* (31), 5130-5143.
54. Zhang, J.; Zhou, Y.; Zhu, Z.; Ge, Z.; Liu, S., Polyion Complex Micelles Possessing Thermoresponsive Coronas and Their Covalent Core Stabilization via “Click” Chemistry. *Macromolecules* **2008,** *41* (4), 1444-1454.